



RESEARCH ARTICLE - PHYSICS

Preparation of Pure ZnO and CNP/ZnO nanostructures as Efficient Bio Sensor

Mohamad Yahya Zuaiter¹, Osama Abdul Azeez Dakhil²

^{1,2}Department of Physics, College of Science, Mustansiriyah University, Baghdad, Iraq

¹Corresponding author E-mail: mohamad.yahya@uomustansiriyah.edu.iq

²dr.osama@uomustansiriyah.edu.iq

Article Info.	Abstract
<p><i>Article history:</i></p> <p>Received 24 September 2024</p> <p>Accepted 7 October 2024</p> <p>Publishing 30 March 2026</p>	<p>This work presents the production of pure zinc oxide (ZnO) films and carbon nanoparticle (CNP) decorated ZnO (CNP/ZnO) nanostructured films for glucose sensors, this study describes a potentially useful method. Carbon nanoparticles were created via the hydrothermal process, and zinc oxide nanoparticles with an average particle size of 11.14 nm were grown on zinc foil using the anodization method. Using the ultrasonication method, carbon nanoparticles were decorated on ZnO film nanocomposites. Numerous experiments were conducted, such as the examination of the microstructure, the analysis of crystallinity, and the study of electrochemical properties. Photoluminescence (PL) measurements, energy-dispersive X-ray spectroscopy (EDX), field-emission scanning electron microscopy (FE-SEM), transmission electron microscopy (TEM), UV-vis spectroscopy, and X-ray diffraction (XRD) were the methods used to determine the nanostructures. When the CNPs/ZnO nanostructures were compared to pure zinc oxide nanostructures, the electrochemical analysis of the former greatly improved the sensitivity to glucose. Using a linear range of 0.3 mM to 1 mM and a low detection limit of 1.15 mM, the CNP/ZnO nanostructures improved glucose sensing with a sensitivity of 2372 $\mu\text{A.mM}^{-1}\text{cm}^{-2}$.</p>

This is an open-access article under the CC BY 4.0 license (<http://creativecommons.org/licenses/by/4.0/>)

The official journal published by the College of Education at Mustansiriya University

Keywords: Glucose Sensors, ZnO biosensors, Anodization technique, Carbon nanoparticles, hydrothermal method

Introduction

One of the main causes of death worldwide is diabetes, which is more commonly defined as an abnormally high blood glucose level. Blood glucose monitoring is necessary to identify and prevent the onset of this potentially fatal condition [1, 2], clinically significant benefits can be obtained from quantitative blood glucose monitoring, which lowers the risk of diabetes mellitus-related heart disease, renal failure, and blindness [3-5]. Since blood glucose imbalance is the primary cause of diabetes mellitus, a serious global public health issue, glucose monitoring with sensors is an area of intense research activity. Research has indicated that dietary modifications and rising rates of obesity can cause blood glucose levels to increase [6, 7]. A wide range of technologies spanning multiple industries, including nanomaterials, medicine, devices, fabrication, electronics, communication, and energy, are included in the field of nanotechnology, which is not a single technology or discipline. It involves having the capacity to measure and manipulate matter at the nanoscale. Nanotechnology is the creation and modification of materials down to 10^{-9} m in size [8]. Nanomaterials are being created in new ways, and as their unique qualities are gradually revealed, so too have their uses in biosensors advanced significantly. To detect and manipulate atoms and molecules, for instance, nanomaterials-based biosensors—that combine material science, molecular engineering, chemistry, and biotechnology—can significantly increase the sensitivity and specificity of biomolecule detection. They also hold great promise for use in pathogenic diagnosis, environment monitoring, and biomolecular recognition [9, 10]. A biological response can be transformed into an electrical signal by analytical devices called biosensors. Biosensors require a high degree of specificity [11]. Biosensors are essential analytical tools for the targeted identification of various analyses. A target biomolecule and a transducer, which converts the biological interaction into a physical signal (optical, chemical, electrical, thermal, etc.), are both present in the biosensor's bioselective layer [12, 13].

As a subclass of chemical sensors, electrochemical biosensors combine the high specificity of biological sensors with the sensitivity of electrochemical transducers, as demonstrated by their low detection limits recognition mechanisms [14]. Electrochemical sensors can be broadly classified into two categories: enzymatic and non-enzymatic, based on the detection mechanism. In 1962, Clark and Lyons presented an enzyme electrode that used the enzyme glucose oxidase for the first time. An enzyme's ability to sense glucose (such as glucose oxidase or glucose dehydrogenase) is dependent on the process of glucose oxidation, which produces hydrogen peroxide and gluconolactone [15, 16]. The first enzymatic glucose sensors were introduced by Clark and Lyons in 1962, for over two decades, the glucose sensor industry has been dominated by enzymatic glucose biosensors. However, several significant issues prevent it from developing further. Enzymatic sensors are not suitable for continuous monitoring applications due to their lack of chemical and thermal stability and their high cost [17].

The composition and morphology of the sensor can significantly alter its sensing properties, making the fabrication of high-performance enzyme-less glucose sensors challenging. These sensors necessitate research into suitable structures to enhance the sensing properties [18]. Direct electrocatalytic oxidation-based enzyme-less glucose sensors are a potent way to solve enzymatic issues. For measuring glucose, a non-enzymatic sensor with high stability, ease of use and durability must be designed [19, 20]. Because of their potential in medical treatment, non-enzymatic glucose biosensors—that initiate glucose oxidation without the need for glucose oxidase (GOx)—have garnered a lot of attention recently. Specifically, these biosensors possess characteristics that can mitigate significant shortcomings of enzymatic sensors, such as their reliance on external factors (temperature, pH, humidity, etc.), their lack of economic viability, and the intricate processes involved in enzyme immobilization [21].

Nanostructured metal oxides, or NMOs, have gained prominence recently as materials that effectively immobilize biomolecules with the right orientation, improved conformation, and high biological activity, leading to improved sensing properties. Interfacing bio-recognition components with transducers for signal amplification can be made interesting by using nanostructured metal oxides, which have desirable functionalities and surface charge properties in addition to unique optical, electrical, and molecular properties [22, 23]. Thought about Zinc oxide (ZnO) is an n-type semiconductor that is particularly inexpensive, non-toxic, and simple to make. Its excellent optical and electrical characteristics have demonstrated significant benefits for biomolecule detection applications involving non-enzymatic sensors. Furthermore, ZnO nanostructured materials can effectively increase the electro-catalytic glucose response due to their larger scale. ZnO nanostructures are said to be able to offer a sufficiently large surface area for surface modification by other materials [24-26]. Moreover, ZnO nanostructures can be readily surface-functionalized and interfaced with chemical and biological substances at different pH and temperature levels due to their biocompatible nature [27, 28].

A more modern class of nanomaterials, carbon nanoparticles (CNPs), is based on carbon sp² atoms in the inner core. These novel Nano-dots have a broad range of applications, including molecular communication, bio imaging, theranostic, bio sensing, and analytical. However, using them as Nano catalysts is a relatively recent development [29]. Anodization is a technique with a lot of potential because it can produce a wide range of morphologies. By adjusting the type of electrolyte, voltage, temperature, and reaction time, it is also possible to control the size and density of the nanostructures through this electrochemical process. Anodizing zinc resulted in the formation of various nanostructures, such as Nano porous-like structures, Nano flakes, micro tip, stripe-like nanostructures, nanocrystals, nanoparticles, Nano flowers, Nano needles, and nanowires [30-32] one of the most popular techniques for creating nanomaterials is hydrothermal synthesis. In essence, it is a solution-reaction-based methodology. The formation of nanomaterials in hydrothermal synthesis can occur at temperatures ranging from room temperature to extremely high temperatures.

Depending on the vapor pressure of the primary component in the reaction, low-pressure or high-pressure conditions can be used to control the morphology of the materials to be prepared. This method has been effectively applied to the synthesis of numerous kinds of nanomaterials. The hydrothermal synthesis method has several advantages over other methods [33-35].

The novelty in the work is the manufacture of a nanomaterial of zinc oxide decorated with carbon nanoparticles that act as an electrode to detect and determine the presence of glucose.

Experimental Part

Synthesis ZnO NPs by Anodization Method

Every electrochemical experiment was carried out at room temperature using zinc foil that had a high purity (99.99%) and thickness (250 μ m) that was obtained from (BDH Company). It is cut into 1 cm by 1 cm pieces and cleaned by submerging it in a solution made of 10 ml of pure (99.7%) ethanol (C₂H₅OH) produced by (ALPHA CHEMIKA) and 5 ml of acetone (C₃H₆O) produced by (ALPHA CHEMIKA). The beaker is then placed in the ultrasonic device (JEKEN PS-30, China) for 15 minutes, after which it is cleaned with DI water and dried. The anodizing process was carried out by dissolving 1 M NaOH produced by Schlau (Spain) in 50 ml DI water and stirring it for five minutes in a magnetic stirrer hotplate (STUART SCIENTIFIC, UK). In a homemade Teflon cell. Zn sheet is the working electrode and the graphite electrode is the counter. A 20 mm gap has been installed between the electrodes, and both electrodes are immersed in NaOH solution. During thirty minutes, six volts were used for the anodization process. The Zn sheet surface developed a light layer because of the reaction, which was then removed from the solution and dried. The anodized ZnO films were then annealed at 200 °C for two hours, which resulted in the appearance of a dark gray layer on the Zn substrate surface, Fig (1) shows a Schematic of the system of the process.

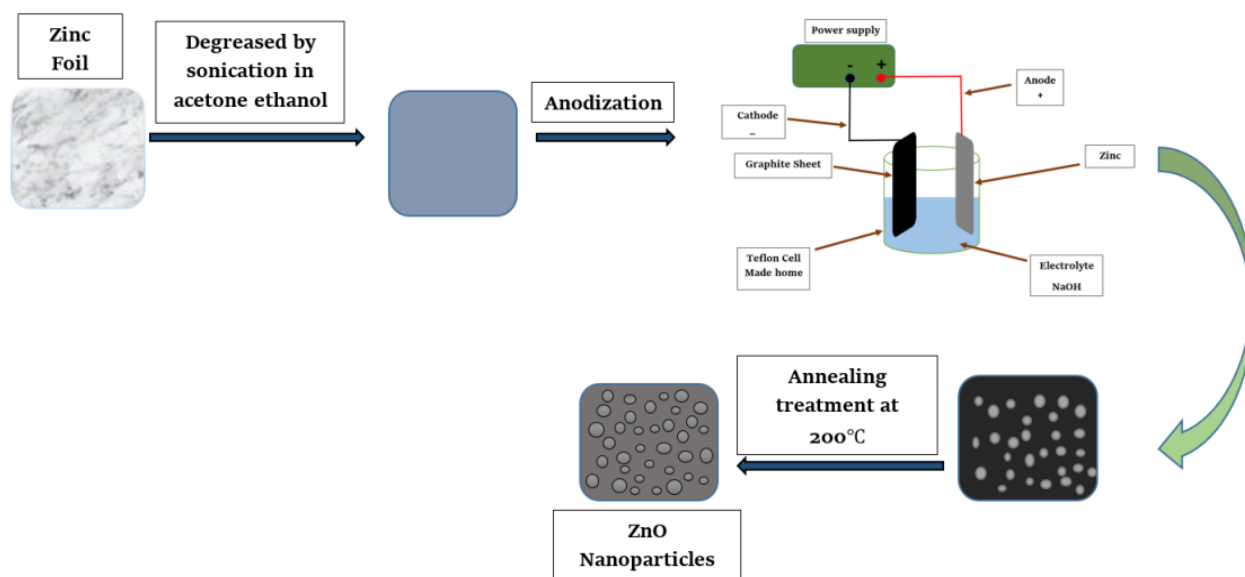


Figure 1 Anodizing system setup

Synthesis of Carbon Nanoparticles (CNPs) by Hydrothermal

The process used to produce CNPs involved dissolving 0.1 M of ascorbic acid from China in 160 ml of DI water, stirring it for 10 minutes in a magnetic stirrer hotplate from STUART SCIENTIFIC, UK, and then applying it in a stainless steel autoclave and applying it in a box furnace

(CARBOLITE, ENGLAND) for 6 hours at 180°C. A schematic of the hydrothermal technique used to prepare carbon nanoparticles is shown in Fig (2).

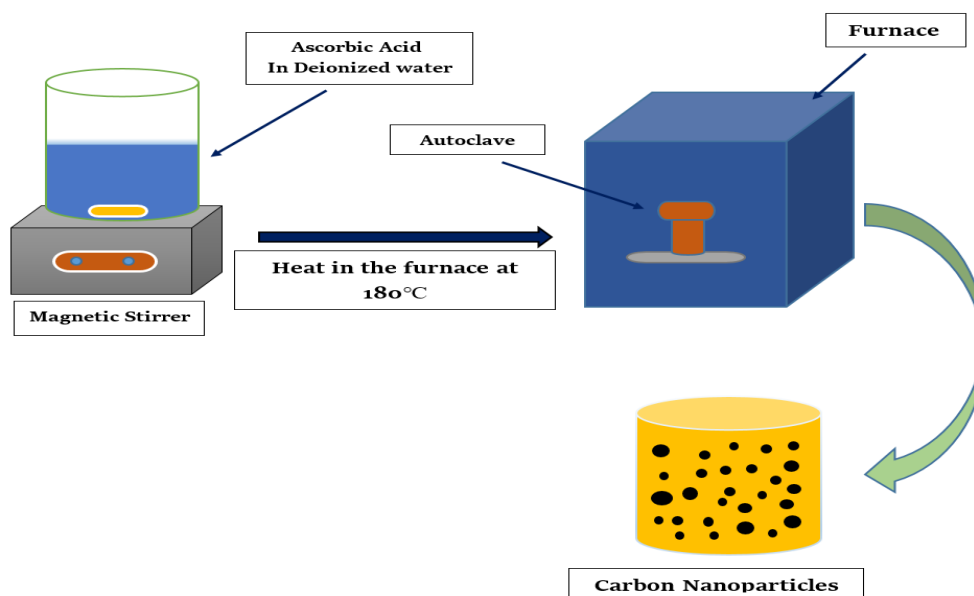


Figure 2 The hydrothermal technique to syntheses CNPs

Preparation ZnO/CNP by Ultrasonic Method

The carbon nanoparticle-containing liquid into a petri dish, then add the ZnO sample so that it is completely submerged in the liquid. Then, place the petri dish inside the ultrasonic machine and leave it there for five minutes. Fig (3) illustrates how to prepare the surface decoration of ZnO foil with carbon nanoparticles using the ultrasonic method

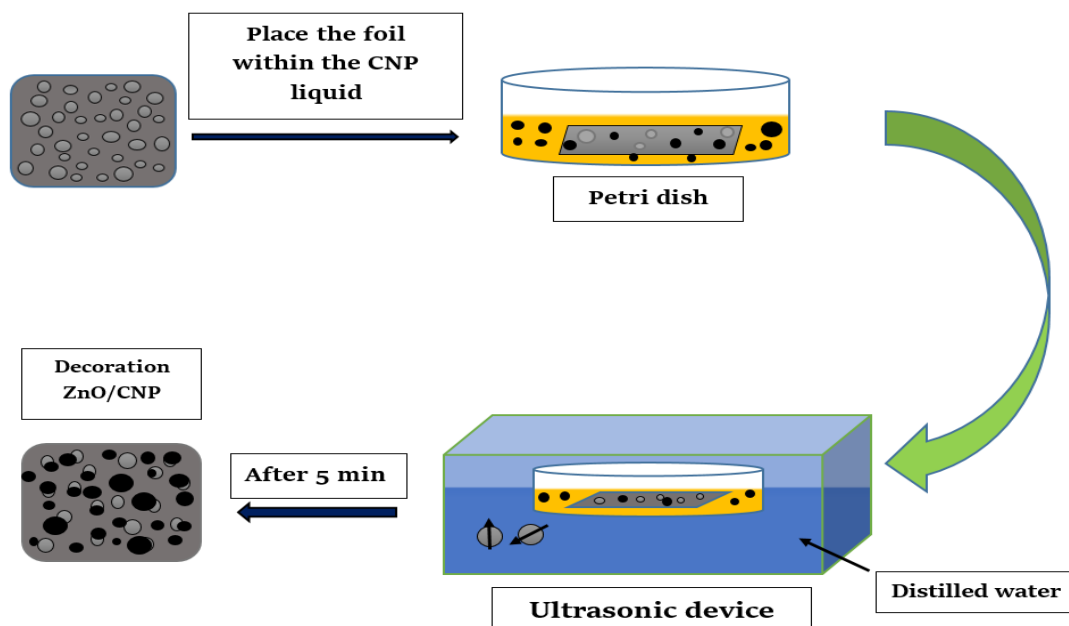


Figure 3 Diagram showing the preparation of ZnO foil's surface decoration with carbon nanoparticles using the ultrasonic technique

Characterization

A variety of tools were used to describe the characteristics of the prepared films. Using a $\text{CuK}\alpha$ radiation source and origin ($\lambda = 1.5418 \text{ \AA}$), X-ray patterns from the deposited films were acquired using a Bruker D8 Advance diffractometer. Energy Dispersive Spectroscopy (EDX) was used to determine the elemental composition of the materials, and the structural properties and morphology were investigated using a Field-Emission Scanning Electron Microscopy (FESEM) model Mira3 Tescan from (Czech).

Electrochemical Measurements

A Keithley 2430-C Source Meter (SMU) instrument (A Tektronix Company) with a contact check/GPIB interface and a 1 kW pulse mode was used to perform the electrochemical measurements shown in Fig (4). For all electrochemical experiments, a three-electrode device consisting of a working electrode (WE), a counter electrode (CE), and a reference electrode (RE) was employed. Ag/AgCl serves as the reference electrode, graphite sheets serve as the counter electrode, and the prepared ZnO nanoparticles serve as the working electrode. When the chronoamperometric responses of pure ZnO were examined at 1 V, the electrodes were at room temperature. Cycle voltammetry (CV) and IV were used to characterize electrodes in 0.1M (NaOH) (supporting electrolyte) at a scan rate of 100 mV with different concentrations of glucose (0.3, 0.5, 0.7, 0.9, and 1 mM). ZnO NPs' chronoamperometric responses were evaluated at 1 V. To ensure reproducibility, each experiment was run at room temperature and at least four times. The electrodes' air temperature was maintained consistently.

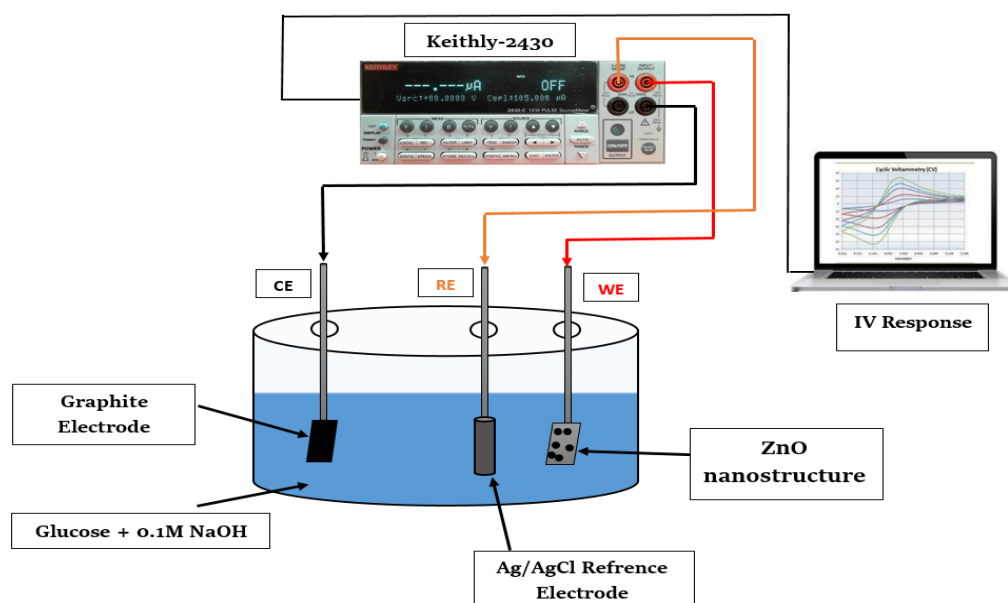


Figure 4 Diagram showing the measuring system of glucose biosensor electrodes

Results and Discussion

In this section, the results are presented and discussed.

X-ray Diffraction (XRD) Analysis

XRD patterns were used to identify the phases and analyze the structural properties of ZnOs and CNP/ZnO. In the experiment, comparisons between patterns were done. ZnO's diffraction peaks are

precisely indexed and hexagonal according to the Joint Committee on Powder Diffraction Standard database (JCPDS). ZnO (36-1451) found that the seven peaks of ZnO nanostructures matched the hkl Miller indices of the crystallographic ZnO planes of (002), (101), (102), (110), (103), (112), and (202), respectively. The peaks were located at (34.86°, 36.84°, 47.97°, 57.22°, 63.29°, 68.33°, and 77.99°) [36]. Scherer equation [37].was employed to evaluate the crystallite size (D) of the prepared films :

$$D = \frac{0.9 \lambda}{\beta \cos \theta} \quad (1)$$

D is the size of the crystallite, λ is the wavelength, (β) is the full-width half-maximum of the peak (FWHM), and (θ) is the Braggs angle where the thick film experiences microstrain and dislocations as a result of the heat treatment process. The density of dislocations (δ) [38]. Can be calculated according to the equation:

$$\delta = \frac{1}{D^2} \quad (2)$$

The film microstrain (ε) [37]. Was calculated using the equation:

$$\varepsilon = \frac{\beta \cos(\theta)}{4} \quad (3)$$

Using Scherer's formula (1), the crystallite sizes were estimated and found to be ranging from 5 to 14 nm in size. Table (1) displays the XRD peak position (2θ), diffraction planes (h k l), lattice parameters (d), FWHM, the crystallite size (D), dislocation density (δ), and strain (ε) of ZnO NPs. Fig (5) displays the XRD patterns of the Pure ZnO CNP/ZnO and Carbon nanoparticles. It can be observed from the above XRD pattern that the average crystallite size of ZnO nanostructures is 9.56 nm.

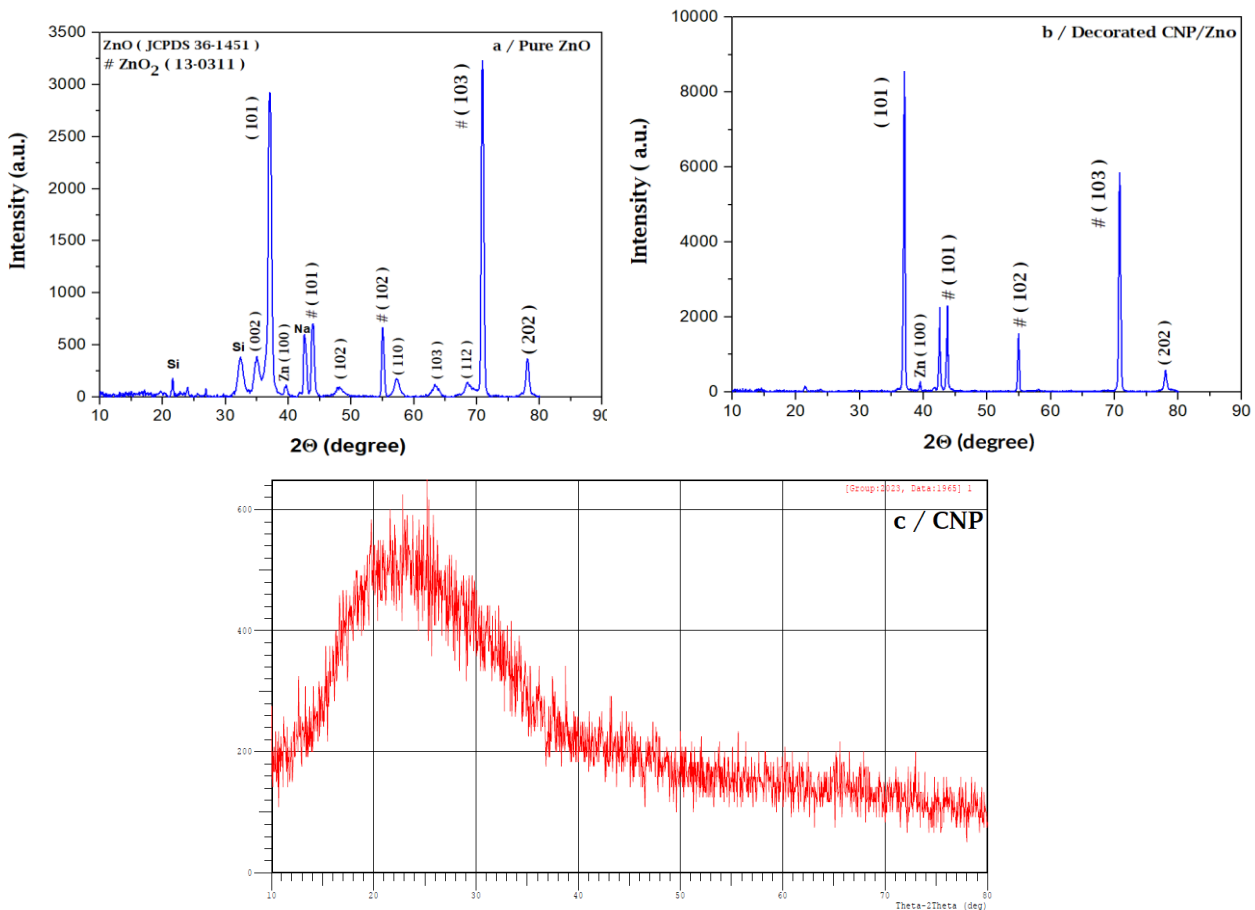


Figure 5 XRD patterns of the a- Pure ZnO b- Decorated CNP/ZnO c- CNP

Table 1. XRD peak position (2θ), diffraction planes (h k l), lattice parameters (d), FWHM, the crystallite size (D), dislocation density (δ), and the strain (ϵ) of ZnO NPs and ZnO₂.

Mat	2θ Exp	2θ JCPDS	θ radians	d (Å°)	hkl	FWHM radians	ϵ (10^{-3})	δ cm^{-2} (10^{10})	D nm
ZnO	34.86	34.42	0.305	2.603	002	0.0113	2.82	66.3	12.28
	36.84	36.25	0.322	2.428	101	0.0104	2.59	56.1	13.34
	47.97	47.53	0.418	1.911	102	0.0175	4.37	159	7.93
	57.22	56.60	0.499	1.624	110	0.0187	4.67	181.6	7.42
	63.29	62.86	0.551	1.477	103	0.0185	4.62	177.7	7.50
	68.33	67.96	0.595	1.378	112	0.0271	6.76	381.4	5.12
	77.99	76.95	0.680	1.238	202	0.0104	2.59	56.1	13.34

The EDX Analysis of ZnO Nanoparticles

Fig (6), reveals the result of the examination of the energy-dispersing X-ray spectrum showing the presence of zinc and oxygen, and the proportions of weight of Zn and O, which are 81.34 % and 18.66 %, respectively, and in the figure, it appears the result of the examination of the energy-dispersing X-ray spectrum shows the presence of zinc and oxygen and Carbon, and the weight percentages of Zn and O and C, which are 59.76 % and 19.43 % and 20.81 %, respectively, This confirms the adsorption of carbon nanoparticles on the surface of zinc oxide Nanoparticles

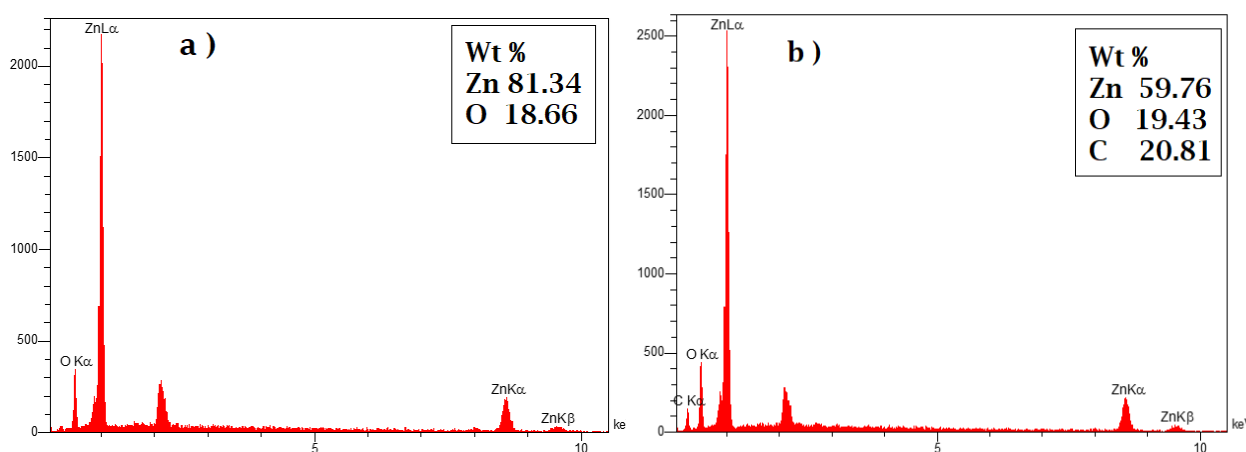


Figure 6 The EDX analysis a- Pure ZnO b - Decorated CNP/ZnO

Morphological Analysis

Fig (7) depicts FE-SEM images. At a magnification of 200 nanometers, It is noticed that zinc oxide nanoparticles were created in diameters ranging from (7.98 – 16.02) nm, the average is about (11.14) nm, and Figure (b), images at 200 nm magnification demonstrate how the zinc oxide layer became after being adorned with carbon nanoparticles. It should be observed that the carbon nanoparticles sheet has become a single layer without features above the zinc oxide layer due to its

pH value of (3), indicating that it is acidic. It was discovered that carbon nanoparticles cover the majority of the surface of zinc Foil.

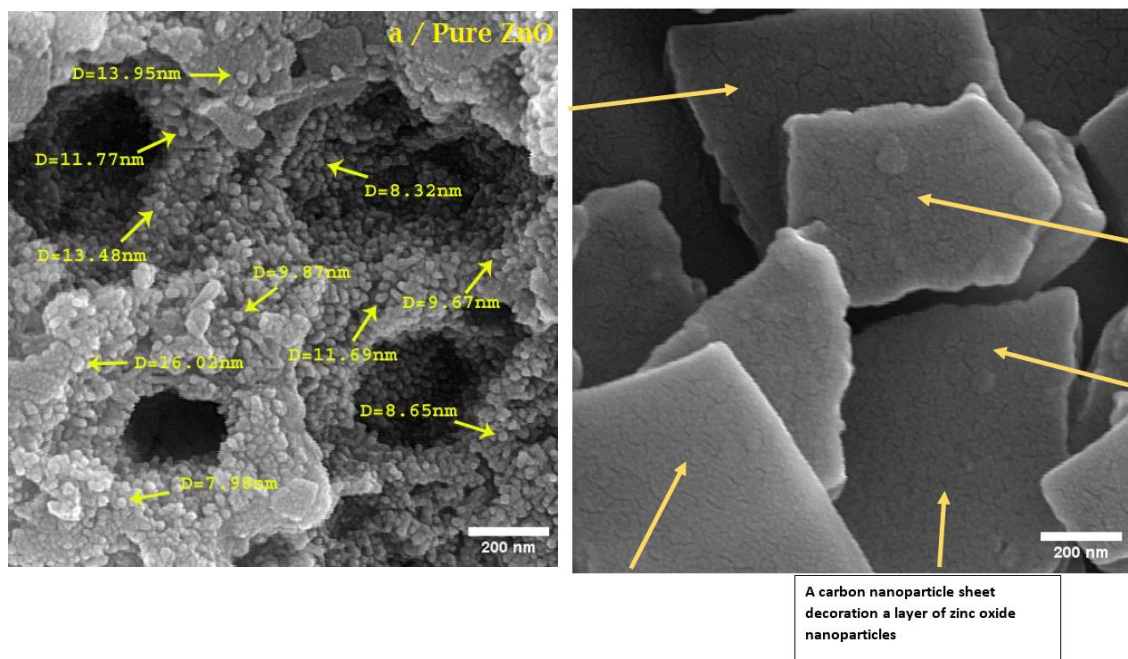


Figure 7 The morphology images of a- Pure ZnO b – Decorated CNP/ZnO

TEM (Transmission electron microscopy) Morphological Analysis

TEM images at magnification ranging from approximately 25 nm to 80 nm are shown in Fig. (8). Analysis reveals the formation of carbon nanoparticles.

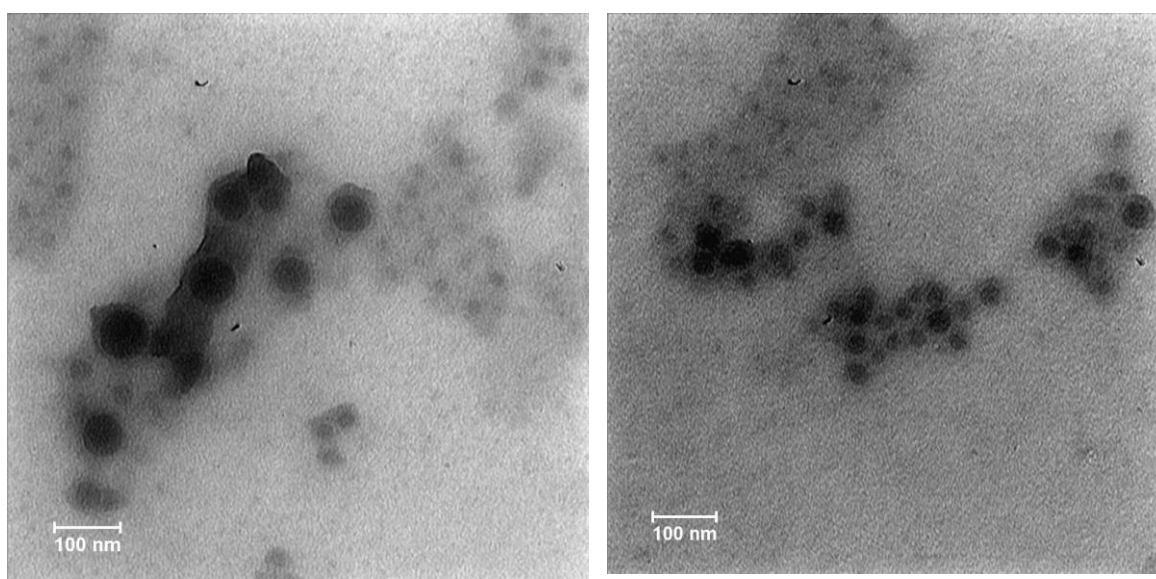


Figure 8 TEM images at magnification almost from (25 nm to 80 nm)

Photoluminescence (PL) Measurements

Fig. (9) shows The spectrum of PL of the pure ZnO and CNP/ZnO were carried out with an excitation wavelength of 350 nm and showed a distinct peak at 355.3 nm and 365.4 nm, respectively, pointing to a better absorbent substance for sensor applications By using of Planck's equation ($E_g = hc/(\lambda)$), the energy band gap of ZnO, CNP/ZnO could be estimated, were calculate and found to be 3.49 eV, 3.39 eV, respectively. The band gap shift observed in various nanomaterials may be attributed to electron limitations, as documented in those materials, as well as variations in morphological features, defects, and grain size restriction, leading to highly efficient material for glucose biosensors [38].

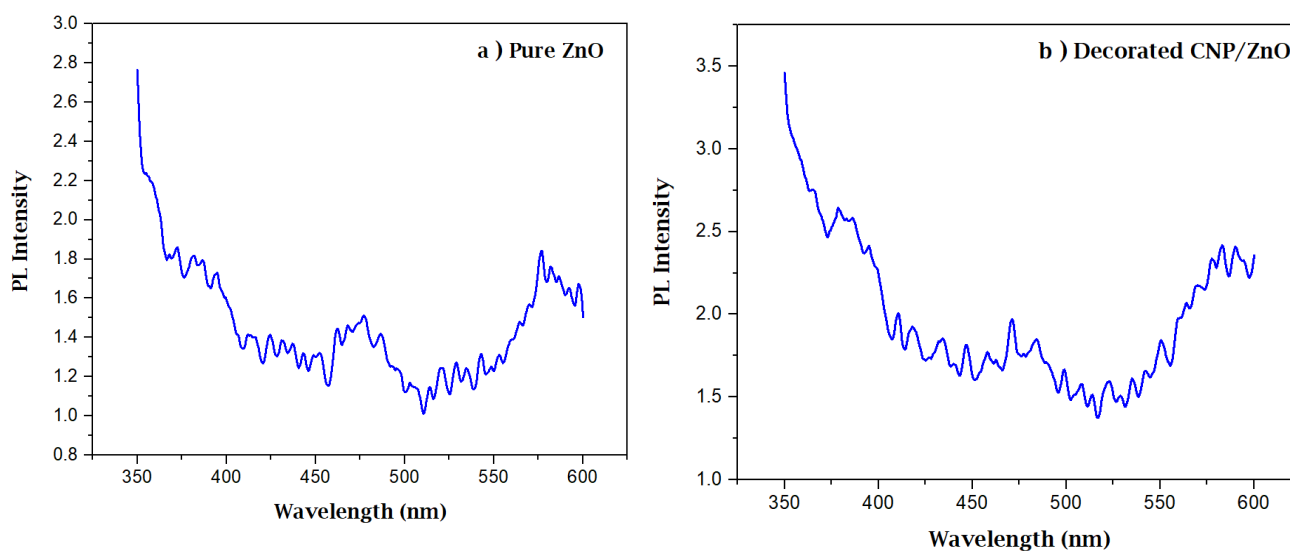


Figure 9 PL spectra of the Zinc oxide nanostructures a – pure ZnO b – Decorated CNP/ZnO

UV–Vis Spectra Analyses

Fig. 10 illustrates the absorption edge of the UV-vis spectrum of CNPs, which is attributed to direct electron transitions between the valence and conduction bands at 465 nm. Figure (11) displays the band gap energy of CNP, which is determined to be (2.6 eV). This shift in band gap between ZnO, CNP/ZnO, and CNPs can be caused by the various morphological characteristics, defects, and constriction of grain size of each, as well as the electron limitations that have been reported in a variety of nanomaterials

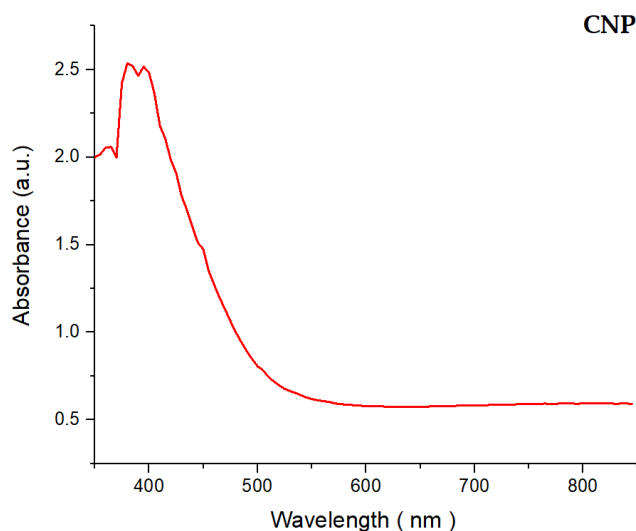


Figure 10 Absorption spectra of CNP

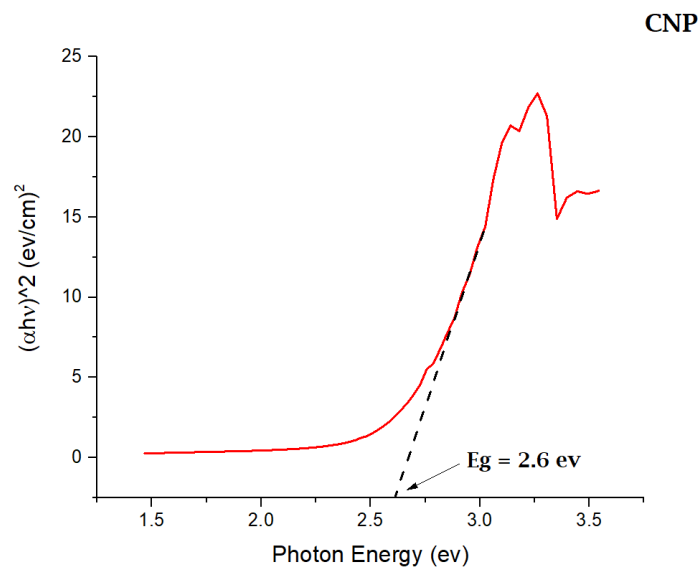


Figure 11 Energy band gap of CNP

The Glucose Biosensor's Electrochemical Characterization

The main features and functionalities of the proposed biosensor were assessed to ascertain how well it could carry out high-accuracy measurements by looking at and analyzing the electrical response of the glucose biosensor. By looking at and analyzing their IV characteristics, electrode sensors' electrical responsiveness can be increased, making it possible to estimate their sensitivity. The variety of glucose molarities was chosen because, as the concentration grows, the sensor's sensitivity increases. Generally, IV characteristic curves are used to mathematically and electrically characterize the behavior of various biosensor components inside an electronic circuit. Therefore, the current responsiveness of biosensors can be recorded via the applied voltage (0 – 1) V with a scan rate of 100 mV/s, utilizing low glucose molarity to determine the sensor's sensitivity at low concentrations, in the different concentrations within the range of (0 – 0.3 – 0.5 – 0.7 – 0.9 – 1) mM dissolved in the NaOH aqueous solution. The effective conductivity of ZnO nanoparticles and CNP/ZnO nanostructures at varying concentrations for the working electrode is displayed in Fig (12). All measurements were taken at room temperature. The manufactured glucose sensor exhibits a significant increase in current when exposed to a voltage between 0 and 1 volts. Additionally, an increase in current was observed with an increase in glucose concentration. There are no peaks and just a slight background current at zero glucose concentration. On the other hand, the maximum glucose biosensor response, the highest current, and the 1 mM glucose concentration were all reached by increasing the concentration. By using the slope of the linear line drawn for the measured response current, the sensitivities of the bare ZnO NPs and CNP-decorated ZnO NPs sensors were assessed. The sensor reacts well to lower glucose concentrations. Reusability, reproducibility, and stability are other important aspects to consider when evaluating the efficacy of sensing apparatus.

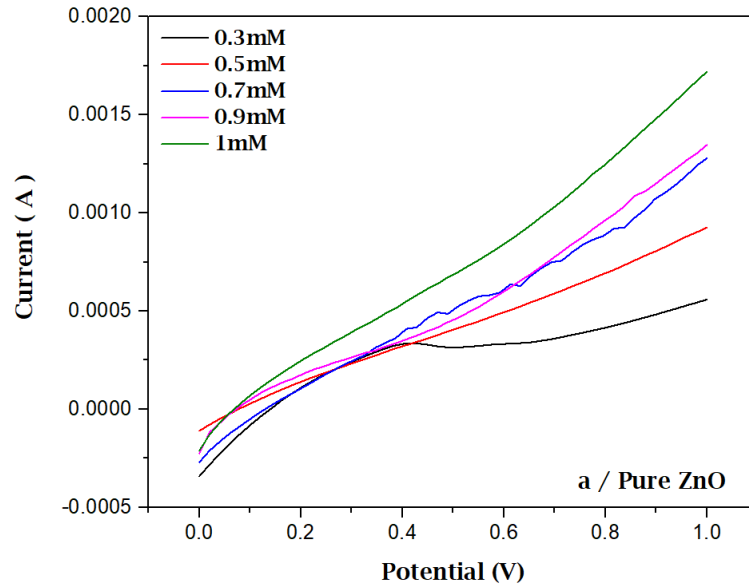


Figure 12 a) IV Characterization of Pure ZnO with different glucose

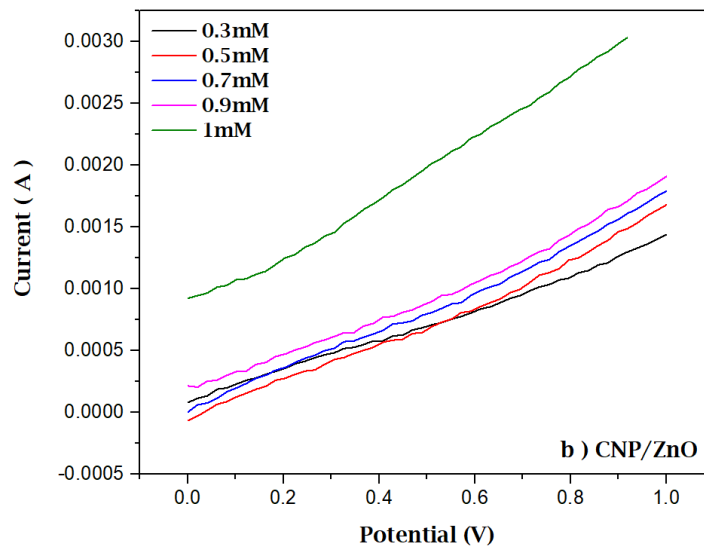


Figure 12 b) IV Characterization of CNP/ZnO with different glucose

The Keithley 2430-C was used to measure the cycle voltammetry (CV) of Pure ZnO NPs and decorative CNP/ZnO Nanostructures generated by the anodization process at a voltage of 6V for 0.5 hours. Measurements were carried out with different concentrations within the range of (0, 0.3, 0.5, 0.7, 0.9, 1) mM glucose dissolved in 0.1M of the NaOH aqueous solution. The potential ranged from -2 to 2 V. Fig (13) shows the CV response of ZnO NPs and CNP/ZnO nanostructure electrodes to glucose. The peak current density of the CNP/ZnO sample was found to be larger than that of pure ZnO NPs. The figure also shows that oxidation and reduction were achieved, and the peaks were symmetric. When glucose was introduced to the electrolyte, the oxidation peak current density differed between samples. The observation revealed a substantial oxidation peak, peaking at around 1.76 V. It is noted that when glucose concentrations increase, the peak current increases, showing that the electrode's ability to oxidize glucose has improved, corresponding to the glucose electro-oxidation occurring at the electrode's surface.

Carbon nanoparticles immediately coated on the electrode's surface provided the sensor with excellent mechanical stability while also contributing to the electrode's extraordinary stability, resulting in increased sensitivity. The sensor's sensitivity is defined by the number of electrons released into the electrolyte during the electrochemical reaction. When glucose levels grow linearly, the curve's intercept and gradient in Fig (14) demonstrate a sensitivity of $1606 \mu\text{A}/\text{mM}\cdot\text{cm}^2$ Using a ZnO nanoparticles sheet as an electrode results in a sensitivity of $2372 \mu\text{A}/\text{mM}\cdot\text{cm}^2$ compared to CNP/ZnO nanostructures With a low limit of detection (0.4 and 1.15 mM, respectively). The enhanced ZnO/CNP electrode accelerates the glucose electrochemical reaction, resulting in a higher sensitivity value due to the synergistic effect of ZnO and CNP.

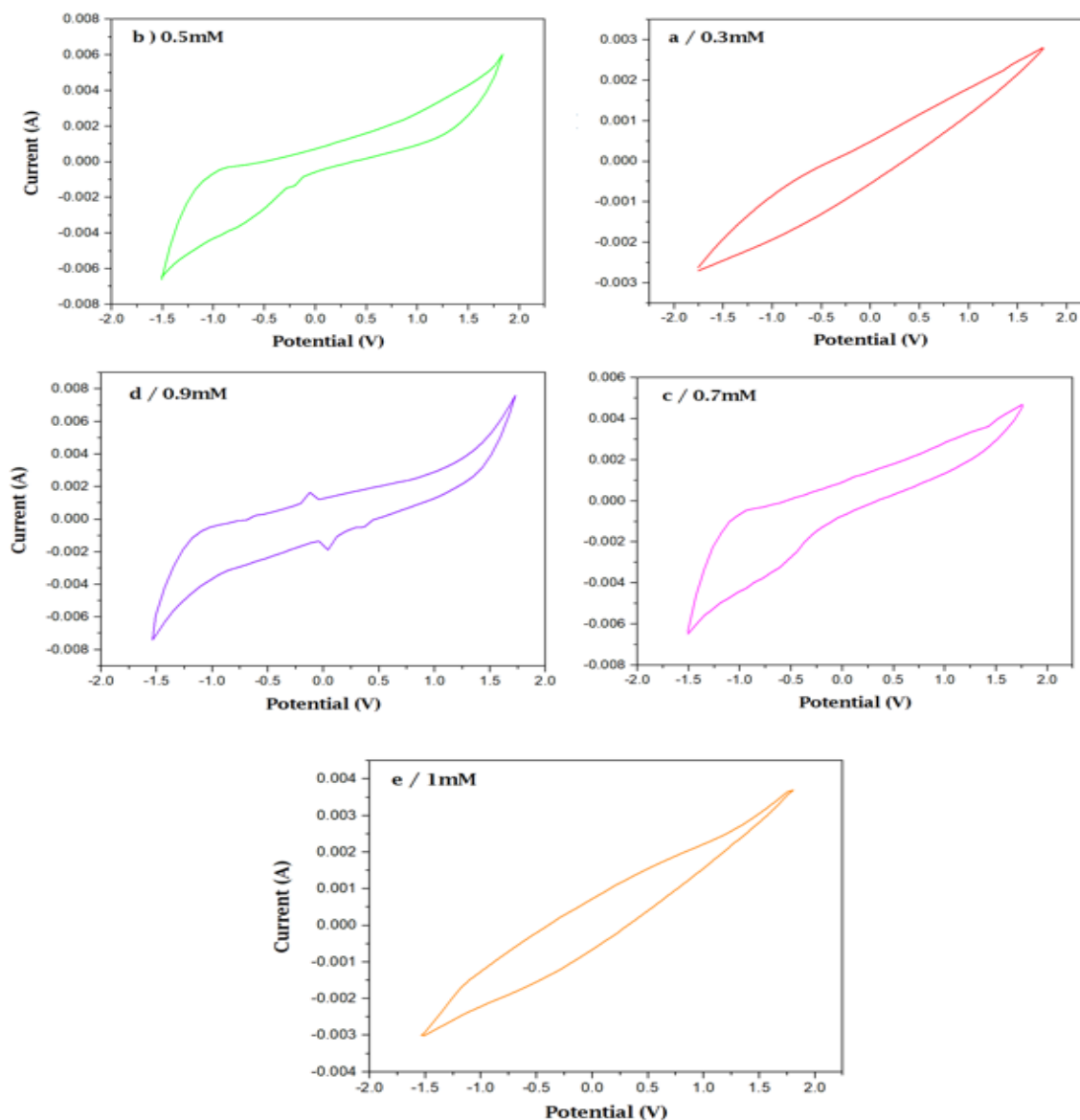


Figure 13 a / CV of ZnO at different concentrations of Glucose (a) 0.3mM (b) 0.5mM (c) 0.7mM (d) 0.9mM (e) 1mM

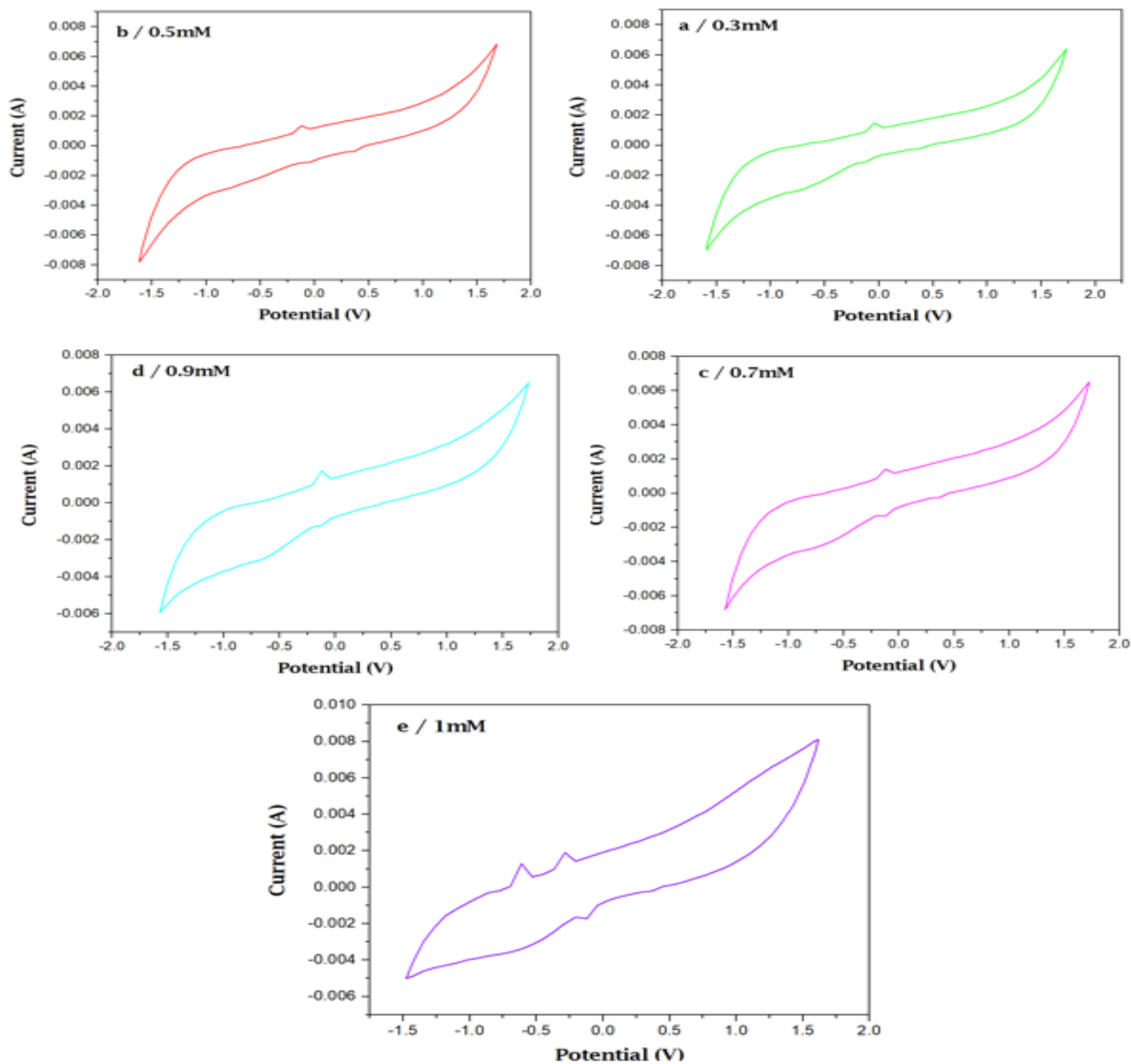


Figure 13 b/ CV of CNP/ZnO at different concentrations of Glucose (a) 0.3mM (b) 0.5mM (c) 0.7mM (d) 0.9mM (e) 1mM

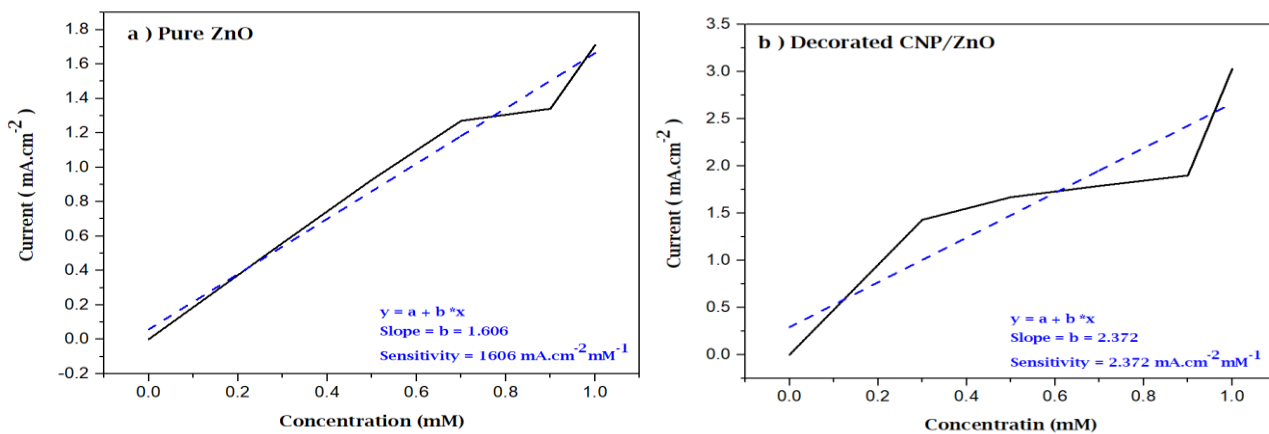


Figure 14 a calibration curve with electrode response a- Pure ZnO b-CNP/ZnO

The present study's sensitivity, detection limit, and linear working range are compared to those of previous glucose biosensors that used various ZnO and related support nanostructures; the results are summarized in Table 2.

Table 2: compares several ZnO electrode-based free-enzymatic electrochemical sensors

Electrode	Sensitivity $\mu A cm^{-2} mM^{-1}$	Linear range	Lower Limit Detection	Referen ce
MWCNT/ZnO QDs	9.36	0.1 – 2.5 μM	0.208 μM	[39]
ZnO/MWCNT/GCE	64.29	1 – 10 mM	0.82 mM	[40]
ZnO/CNO	606.64	0.1 – 15 mM	Not mentioned	[41]
ZnO/Ni/rGO	2030	0.0005 - 1.11 mM	0.15 μM	[42]
ZnO/CNP	2372	0.3 – 1 mM	1.15 mM	This Work

Conclusions

The anodization approach proved an effective method to produce pure ZnO and Carbon Decorated ZnO (CNP/ZnO) for non-enzymatic glucose sensing. The ZnO material performed well as an electrocatalytic glucose biosensor, with good sensitivity. Using the constructed CNP/ZnO electrode resulting an increase in sensitivity about 50%. With good stability, reproducibility, and selectivity, several tests were conducted, including microstructure observation, crystallinity analysis, and electrochemical property investigation. The carbon nanoparticle-decorated ZnO nanoparticle surface has promise for developing extremely sensitive, low-cost electrochemical glucose biosensors. As evidenced by this result, the sensor's high-performance non-enzymatic glucose combined with a low-cost, unique architecture has much potential. A comparison was made between the results obtained by examining the glucose ratio using an electrode of pure zinc oxide nanomaterial and an electrode of zinc oxide nanomaterial decorated with carbon nanoparticles. The results showed high efficiency and excellent performance of the decorated electrode compared to the pure. These results indicate promising materials for Glucose sensing.

Acknowledgments

The authors are grateful to the Department of Physics, College of Science, Mustansiriyah University, for their support and assistance. Also, we'd like to express our gratitude to the Lab personnel for their Assistance.

References

- [1] Y.-H. Lin, C. Sivakumar, B. Balraj, G. Murugesan, S. K. Nagarajan, and M.-S. Ho, "Ag-decorated vertically aligned ZnO nanorods for non-enzymatic glucose sensor applications," *Nanomaterials*, vol. 13, p. 754, 2023.
- [2] H. Zhu, L. Li, W. Zhou, Z. Shao, and X. Chen, "Advances in non-enzymatic glucose sensors based on metal oxides," *Journal of Materials Chemistry B*, vol. 4, pp. 7333-7349, 2016.
- [3] C. Chen, Q. Xie, D. Yang, H. Xiao, Y. Fu, Y. Tan, *et al.*, "Recent advances in electrochemical glucose biosensors: a review," *Rsc Advances*, vol. 3, pp. 4473-4491, 2013.

- [4] P. Naderi Asrami, P. Aberoomand Azar, M. Saber Tehrani, and S. A. Mozaffari, "Glucose oxidase/nano-ZnO/thin film deposit FTO as an innovative clinical transducer: a sensitive glucose biosensor," *Frontiers in Chemistry*, vol. 8, p. 503, 2020.
- [5] J. Burrin and C. Price, "Measurement of blood glucose," *Annals of clinical biochemistry*, vol. 22, pp. 327-342, 1985.
- [6] R. Ahmad, M.-S. Ahn, and Y.-B. Hahn, "Fabrication of a non-enzymatic glucose sensor field-effect transistor based on vertically-oriented ZnO nanorods modified with Fe₂O₃," *Electrochemistry Communications*, vol. 77, pp. 107-111, 2017.
- [7] P. Chakraborty, S. Dhar, N. Deka, K. Debnath, and S. P. Mondal, "Non-enzymatic salivary glucose detection using porous CuO nanostructures," *Sensors and Actuators B: Chemical*, vol. 302, p. 127134, 2020.
- [8] S. Pandit, D. Dasgupta, N. Dewan, and A. Prince, "Nanotechnology based biosensors and its application," *The Pharma Innovation*, vol. 5, p. 18, 2016.
- [9] X. Zhang, Q. Guo, and D. Cui, "Recent advances in nanotechnology applied to biosensors," *Sensors*, vol. 9, pp. 1033-1053, 2009.
- [10] A. A. Cargill, "Development of an enzymatic glucose biosensor for applications in wearable sweat-based sensing," Iowa State University, 2016.
- [11] P. Mehrotra, "Biosensors and their applications—A review," *Journal of oral biology and craniofacial research*, vol. 6, pp. 153-159, 2016.
- [12] A. Tereshchenko, M. Bechelany, R. Viter, V. Khranovskyy, V. Smyntyna, N. Starodub, *et al.*, "Optical biosensors based on ZnO nanostructures: advantages and perspectives. A review," *Sensors and Actuators B: Chemical*, vol. 229, pp. 664-677, 2016.
- [13] N. J. Ronkainen, H. B. Halsall, and W. R. Heineman, "Electrochemical biosensors," *Chemical Society Reviews*, vol. 39, pp. 1747-1763, 2010.
- [14] A. S. Shamsabadi, H. Tavanai, M. Ranjbar, A. Farnood, and M. Bazarganipour, "Electrochemical non-enzymatic sensing of glucose by gold nanoparticles incorporated graphene nanofibers," *Materials Today Communications*, vol. 24, p. 100963, 2020.
- [15] M. H. Hassan, C. Vyas, B. Grieve, and P. Bartolo, "Recent advances in enzymatic and non-enzymatic electrochemical glucose sensing," *Sensors*, vol. 21, p. 4672, 2021.
- [16] K. Dhara and D. R. Mahapatra, "Electrochemical nonenzymatic sensing of glucose using advanced nanomaterials," *Microchimica Acta*, vol. 185, pp. 1-32, 2018.
- [17] A. K. Manna, P. Guha, V. J. Solanki, S. Srivastava, and S. Varma, "Non-enzymatic glucose sensing with hybrid nanostructured Cu₂O-ZnO prepared by single-step coelectrodeposition technique," *Journal of Solid State Electrochemistry*, vol. 24, pp. 1647-1658, 2020.
- [18] J. Qian, Y. Wang, J. Pan, Z. Chen, C. Wang, J. Chen, *et al.*, "Non-enzymatic glucose sensor based on ZnO-CeO₂ whiskers," *Materials Chemistry and Physics*, vol. 239, p. 122051, 2020.
- [19] I. Chavez-Urbiola, A. Reséndiz-Jaramillo, F. Willars-Rodriguez, G. Martinez-Saucedo, L. Arriaga, J. Alcantar-Peña, *et al.*, "Glucose biosensor based on a flexible Au/ZnO film to enhance the glucose oxidase catalytic response," *Journal of Electroanalytical Chemistry*, vol. 926, p. 116941, 2022.
- [20] H. H. Mai, V. T. Pham, V. T. Nguyen, C. D. Sai, C. H. Hoang, and T. B. Nguyen, "Non-enzymatic fluorescent biosensor for glucose sensing based on ZnO nanorods," *Journal of Electronic Materials*, vol. 46, pp. 3714-3719, 2017.
- [21] P. R. Solanki, A. Kaushik, V. V. Agrawal, and B. D. Malhotra, "Nanostructured metal oxide-based biosensors," *NPG Asia Materials*, vol. 3, pp. 17-24, 2011.
- [22] Q. Dong, H. Ryu, and Y. Lei, "Metal oxide based non-enzymatic electrochemical sensors for glucose detection," *Electrochimica acta*, vol. 370, p. 137744, 2021.
- [23] C.-E. Cheng, S. Tangsuwanjinda, H.-M. Cheng, and P.-H. Lee, "Copper oxide decorated zinc oxide nanostructures for the production of a non-enzymatic glucose sensor," *Coatings*, vol. 11, p. 936, 2021.
- [24] X. Sun, J. Wang, and A. Wei, "Zinc oxide nanostructured biosensor for glucose detection," *Journal of materials science & technology*, vol. 24, p. 649, 2008.

- [25] S. M. Ali, O. A. Dakhil, and E. H. Hussein, "Comparison Between Photoactivity of ZnO/NiO Nanostructures Synthesized by CBD and Modified-CBD for Rhodamine B Removal," *Sigma*, vol. 28, p. 98.5, 2021.
- [26] N. Tripathy and D. Kim, "Metal oxide modified ZnO nanomaterials for biosensor applications. *Nano Converg* 5 (1): 27," ed, 2018.
- [27] A. B. Djurišić and Y. H. Leung, "Optical properties of ZnO nanostructures," *small*, vol. 2, pp. 944-961, 2006.
- [28] C. Testa, A. Zammataro, A. Pappalardo, and G. T. Sfrazzetto, "Catalysis with carbon nanoparticles," *RSC advances*, vol. 9, pp. 27659-27664, 2019.
- [29] A. Ramirez-Canon, D. O. Miles, P. J. Cameron, and D. Mattia, "Zinc oxide nanostructured films produced via anodization: a rational design approach," *RSC advances*, vol. 3, pp. 25323-25330, 2013.
- [30] C.-C. Wang, A.-Y. Lo, M.-C. Cheng, Y.-S. Chang, H.-C. Shih, F.-S. Shieu, *et al.*, "Zinc oxide nanostructures enhanced photoluminescence by carbon-black nanoparticles in Moiré heterostructures," *Scientific Reports*, vol. 13, p. 9704, 2023.
- [31] Y. X. Gan, A. H. Jayatissa, Z. Yu, X. Chen, and M. Li, "Hydrothermal synthesis of nanomaterials," *Journal of Nanomaterials*, vol. 2020, 2020.
- [32] K. Mika, R. P. Socha, P. Nyga, E. Wiercigroch, K. Malek, M. Jarosz, *et al.*, "Electrochemical synthesis and characterization of dark nanoporous zinc oxide films," *Electrochimica Acta*, vol. 305, pp. 349-359, 2019.
- [33] H. A. Jasim, O. A. A. Dakhil, and A. Maleki, "Synthesis of CuO Nanrods Using Chemical Bath Deposition for a Nonenzymatic Glucose Biosensor," *Al-Mustansiriyah Journal of Science*, vol. 34, pp. 97-103, 2023.
- [34] M. S. Hashim, D. M. Naser, and S. H. Lafta, "Hyperthermia Efficiency of Hydrothermal Synthesized Iron Sulfide Magnetic Nanoparticles," *Mustansiriyah Journal of Pure and Applied Sciences*, vol. 2, pp. 134-144, 2024.
- [35] N. J. G. A. H. Mohammed and A. M. AbdulMajeed, "MgO nanoparticles synthesized using chemical method for Skin cancer cell line (A375) cytotoxic assay," *Mustansiriyah Journal of Pure and Applied Sciences*, vol. 2, pp. 88-95, 2024.
- [36] N. A. Hussain, O. A. Dakhil, and L. Y. Abbas, "Evaluation of the effect of Ag-doping ZnO microstructure on optical and structural properties and application in photocatalytic properties," *Al-Mustansiriyah Journal of Science*, vol. 34, pp. 108-114, 2023.
- [37] R. Saadon and O. A. Azeez, "Chemical route to synthesis hierarchical ZnO thick films for sensor application," *Energy Procedia*, vol. 50, pp. 445-453, 2014.
- [38] R. Sabry and O. AbdulAzeez, "Hydrothermal growth of ZnO nano rods without catalysts in a single step," *Manufacturing Letters*, vol. 2, pp. 69-73, 2014.
- [39] V. Vinoth, G. Subramaniam, S. Anandan, H. Valdés, and P. Manidurai, "Non-enzymatic glucose sensor and photocurrent performance of zinc oxide quantum dots supported multi-walled carbon nanotubes," *Materials Science and Engineering: B*, vol. 265, p. 115036, 2021.
- [40] A. Tarlani, M. Fallah, B. Lotfi, A. Khazraei, S. Golsanamlou, J. Muzart, *et al.*, "New ZnO nanostructures as non-enzymatic glucose biosensors," *Biosensors and Bioelectronics*, vol. 67, pp. 601-607, 2015.
- [41] A. Sharma, A. Agrawal, G. Pandey, S. Kumar, K. Awasthi, and A. Awasthi, "Carbon nano-onion-decorated ZnO composite-based enzyme-less electrochemical biosensing approach for glucose," *ACS omega*, vol. 7, pp. 37748-37756, 2022.
- [42] M. Mazaheri, H. Aashuri, and A. Simchi, "Three-dimensional hybrid graphene/nickel electrodes on zinc oxide nanorod arrays as non-enzymatic glucose biosensors," *Sensors and Actuators B: Chemical*, vol. 251, pp. 462-471, 2017.